Band crossings in the positive-parity high-spin states of ^{83}Rb and ^{85}Y

J. Döring,[1,2] G. D. Johns,[1,*] R. A. Kaye,[1,†] M. A. Riley,[1] and S. L. Tabor[1]
[1]*Department of Physics, Florida State University, Tallahassee, Florida 32306*
[2]*Department of Physics, University of Notre Dame, Notre Dame, Indiana 46556*
(Received 27 January 1999; published 17 June 1999)

Positive-parity high-spin states in the odd-proton nuclei ^{83}Rb and ^{85}Y have been populated via the ^{68}Zn(^{18}O,$p2n$) reaction at 56 MeV and the ^{59}Co(^{28}Si,2p) reaction at 99 MeV up to $(37/2^+)$ and $(33/2^+)$, respectively. In both nuclei band crossings have been observed at a spin of 21/2 and interpreted as resulting from the alignment of a $g_{9/2}$ neutron pair, as in other odd-proton nuclei with 46 neutrons. In the three-quasiparticle high-spin excitations, the observed signature splitting and total Routhian surface calculations indicate that the ^{83}Rb nucleus exhibits a well-deformed near-oblate shape. No second alignment has been observed in the yrast sequence of ^{83}Rb up to a rotational frequency of 0.95 MeV, indicating that for $Z=37$ and an oblate shape the breaking of a $g_{9/2}$ proton pair is energetically expensive. [S0556-2813(99)05307-8]

PACS number(s): 21.10.Re, 23.20.En, 23.20.Lv, 27.50.+e

I. INTRODUCTION

Yrast high-spin states in the transitional Rb ($Z=37$) isotopes with mass numbers 81, 83, and 85 may provide valuable information about the interplay of collective and particle-hole excitations as well as about deformation driving properties of the unpaired nucleons. In ^{85}Rb [1,2], the one-quasiparticle (1qp) yrast sequence of positive parity contains weakly collective $E2$ transitions [$B(E2)\approx 14$ Weisskopf units (W.u.)] while the states above spin $21/2^+$ are connected by fast $M1$ transitions [$B(M1)\approx 0.4-1.2$ W.u.]. Level energies and electromagnetic transition probabilities have been successfully described by spherical shell-model calculations. On the other hand, the positive-parity yrast sequence in ^{81}Rb [3,4] is comprised of collective $E2$ transitions [$B(E2)\approx 66$ W.u.] between states of up to $(37/2^+)$ and the cranked shell model has been used to interpret the collective high-spin states. It was found that the irregularities in the moments of inertia can be well explained by the breakup of a $g_{9/2}$ neutron pair around spin $21/2^+$.

For the transitional nucleus between these limits, ^{83}Rb with 46 neutrons, a fragile competition of collective and particle excitations at high spins is expected but not yet studied. In the heavier $N=46$ nucleus ^{87}Nb [5,6], a weakly collective [$B(E2)\approx 12$ W.u.] 3qp sequence has been identified which is built on a low-lying $21/2^+$ state. The $g_{9/2}$ neutron character of the breaking nucleon pair has been recently verified by magnetic-moment measurements [7,8], and it is supported by the neutron character of the yrast 8^+ states in the adjacent even-even nuclei ^{84}Sr [9,10] and ^{86}Zr [7,11]. Further, for an even heavier $N=46$ isotone, ^{89}Tc [12], multiparticle-hole (spherical shell-model) excitations have been suggested for the description of level energies and branching ratios of transitions between states above spin $21/2^+$. The shell-model description is less successful for the low-lying 1qp $g_{9/2}$ proton excitations which may be influenced by weakly collective excitations.

In general, the low-lying one-quasiproton states in the $N=46$ isotones discussed above exhibit a weakly deformed shape with $|\beta_2|\approx 0.15-0.20$. But the evolution of the nuclear shape at higher angular momenta and excitation energies has not been systematically explored. While detailed experimental results are available from multidetector in-beam experiments for the isotones above the spherical subshell gap at $Z=40$, such as ^{87}Nb and ^{89}Tc, only limited data are known for the high-spin states in nuclei situated just below the gap, such as ^{83}Rb and ^{85}Y.

Previously, the low-lying $9/2^+$ isomer in ^{83}Rb at 42.1 keV [13,14] had been found to be populated by a decay sequence of four transitions. They were observed in coincidence via the (α,2n) and (^{6}Li,3n) reactions at 23 and 25 MeV beam energy [13], respectively. Thus, levels up to a 3727.7 keV state were established with spin and parity assignments given up to the $(21/2^+)$ state at 2860.4 keV [13], just around the expected band-crossing region. Further, lifetimes of 6(1), 1.4(3), and 2.9(7) ps were measured [15] for the $13/2^+$, $17/2^+$, and $21/2^+$ states, respectively, providing evidence for a moderately deformed 1qp structure in ^{83}Rb. A decrease in the $E2$ strengths was found when approaching the $21/2^+$ state which may indicate a possible band-crossing scenario.

To complete the $N=46$ band-crossing systematics, more information about the positive-parity high-spin states in the isotone ^{85}Y ($Z=39$) [16] was needed. Previously, states up to a spin of $(29/2^+)$ were identified in this nucleus, just through the $g_{9/2}$ neutron band-crossing region. To explore the onset of high-spin bands and collectivity in the $N=46$ nuclei below the $Z=40$ gap, and to investigate shape variations, in-beam studies of the nuclei ^{83}Rb and ^{85}Y have been initiated. A thin target coincidence experiment has been performed using heavy-ion projectiles to study the behavior of the odd-proton nucleus ^{83}Rb at high angular momentum, while a thick target experiment previously performed for the study of high-spin states in ^{84}Y [17] was analyzed with regard to ^{85}Y.

*Present address: Los Alamos National Laboratory, Los Alamos, NM 87545.
†Present address: Physics Division, Argonne National Laboratory, Argonne, IL 60439.

II. EXPERIMENTAL PROCEDURE AND RESULTS

A. ^{83}Rb

High-spin states in ^{83}Rb were populated via the ^{68}Zn(^{18}O,$p2n$) reaction at 56 MeV beam energy. The ^{18}O beam was provided by the Florida State University Tandem-Superconducting LINAC facility. The target consisted of a thin Zn foil with a thickness of 0.6 mg/cm^2 and was enriched to 99% in ^{68}Zn. For the detection of the γ rays the Pitt-FSU detector array [18] was used consisting of eight high-purity Compton-suppressed Ge detectors at that time. Each detector had a relative efficiency of about 25%. Two of the detectors were placed at a forward angle of 35°, two at 90°, and four at a backward angle of 145°. Energy and efficiency calibrations were performed with a ^{152}Eu source placed in the target position.

The events were stored on 8 mm tape and analyzed offline. Two different matrices were generated, a triangular matrix with all detector pair combinations and a square matrix where the forward and backward detector events were sorted against the 90° detector events. During this sorting process, the events from the forward and backward detectors were Doppler-shift corrected before storing them into the matrices. The triangular matrix contained about 1.5×10^8 coincidence events and was used for the construction of the level scheme.

The square matrix was used to determine directional correlations of oriented nuclei (DCO) ratios [19,20] according to the equation given in Ref. [21]. The interpretation of these ratios is most straightforward when $E2$ transitions are used as gating transitions. In this case, DCO ratios of about 0.5 are expected for pure $\Delta I=1$ dipole transitions and 1.0 for stretched $E2$ transitions based on the geometry of the Pitt-FSU detector setup. For mixed $\Delta I=1$ transitions, the ratio may vary between 0.3 and 1.8 as a function of the dipole-quadrupole mixing and the amount of nuclear alignment.

Based on the measured coincidence relationships the known level scheme of ^{83}Rb has been extended up to a $(37/2^+)$ state at 8834 keV, as shown in Fig. 1. A key element in constructing the level scheme is the placement of the 970 keV doublet. Both components are in coincidence with each other and with the lowest transitions in the sequence. A typical band-crossing scenario has been identified around spin $21/2^+$ where a new high-spin structure emerges. This new band contains the $\Delta I=2$ transitions at 1132.7, 1323.2, 1597, and 1921 keV.

Two background-corrected coincidence spectra are shown in Fig. 2. For each spectrum, the background correction was performed by subtracting an individual background spectrum which was generated from the same matrix by setting an equal width background gate close to the line of interest. The 1096.0 keV transition is known from previous work [13] to be the $17/2^+\rightarrow13/2^+$ transition. The previously reported transition of the low-lying structure can be seen quite well. The 265 keV gate represents a transition involved in the band-crossing region and was not observed in previous work. From both gates the transitions involved in the extension of the band can be seen. The uppermost transition is extremely weak and has been identified through adding up several clean gates. Part of this spectrum is shown in Fig. 3.

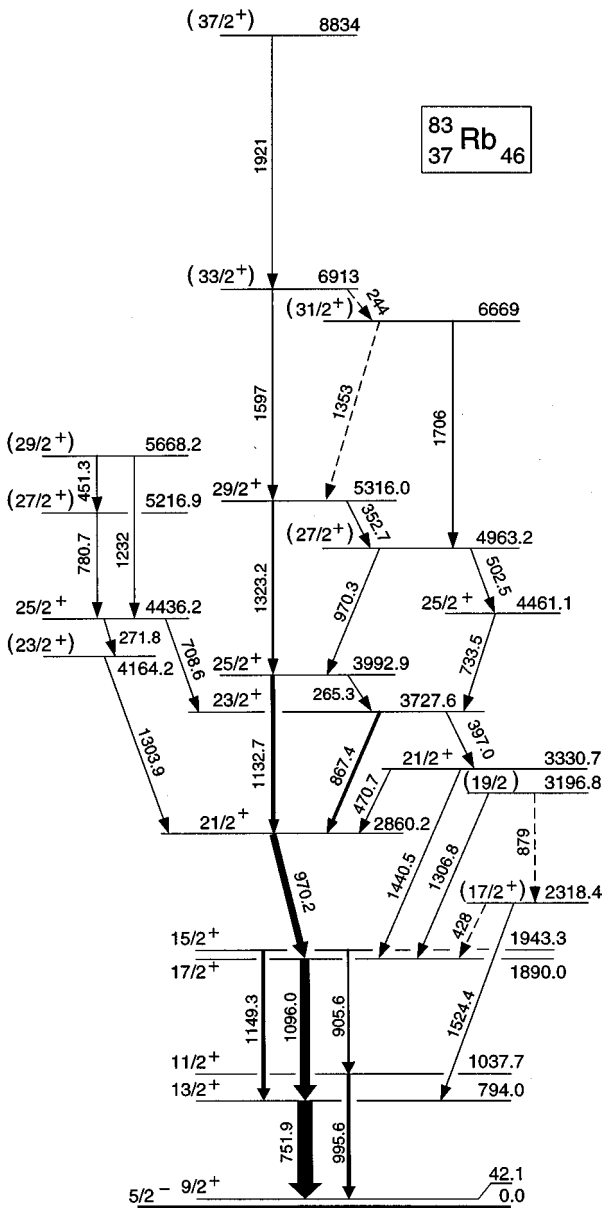

FIG. 1. Level scheme of the positive-parity states in ^{83}Rb as deduced from the present measurement. Spin and parity assignments for the lowest levels have been taken from Refs. [13,14].

Spin assignments, whenever possible, are based on the measured DCO ratios deduced mainly from gates set on the low-lying $E2$ transitions at 752 and 1096 keV (see Table I). In extracting the DCO values, pairs of background-corrected coincidence spectra were generated from the square matrix under identical gate setting conditions for the peak and background gates. The peak areas of the lines of interest were determined by a least-squares fitting procedure to a Gaussian shape. The errors quoted include only statistical uncertainties. Corrections for different detector efficiencies have been estimated to be small for γ-ray energies above 100 keV because of the high degree of symmetry in the Pitt-FSU Ge detector array and, thus, have been neglected. The deduced DCO ratios verify the $\Delta I=2$ nature of the new yrast transi-

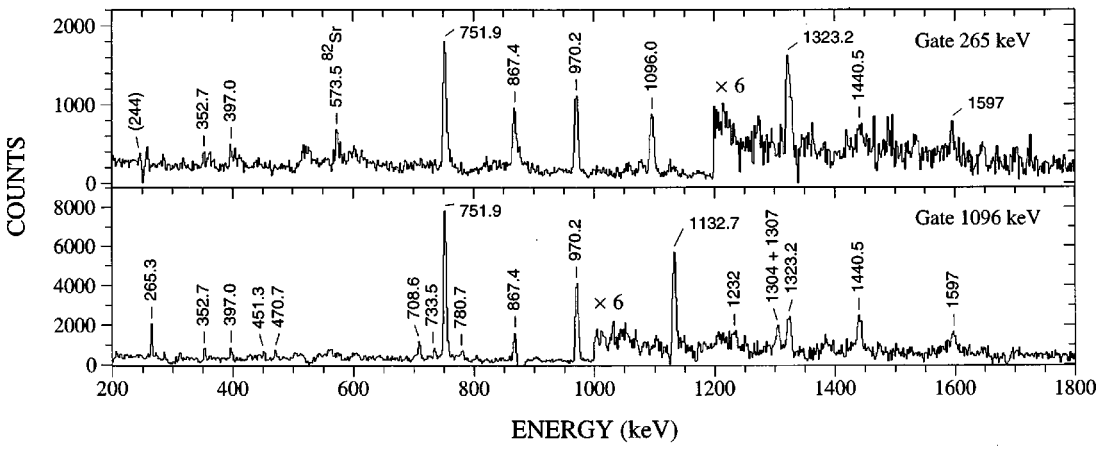

FIG. 2. Background-corrected γ-ray spectra in prompt coincidence with the 265 and 1096 keV transitions.

TABLE I. Energies, relative intensities, and DCO ratios of transitions assigned to ^{83}Rb.

$E_{\rm lev}$[a] (keV)	I_i^π	I_f^π	E_γ[b] (keV)	I_γ	$R_{\rm DCO}$
794.0	$13/2^+$	$9/2^+$	751.9(1)	100(5)[c]	1.04(6)
1037.7	$11/2^+$	$9/2^+$	995.6(1)	20(4)	
1890.0	$17/2^+$	$13/2^+$	1096.0(1)	63(4)	0.91(6)
1943.3	$15/2^+$	$11/2^+$	905.6(2)	5(2)	
		$13/2^+$	1149.3(2)	13(2)	0.54(6)
2318.4	$(17/2^+)$	$17/2^+$	428(1)	2(1)	
		$13/2^+$	1524.4(3)	6(1)	
2860.2	$21/2^+$	$17/2^+$	970.2(1)	50(5)	0.94(5)[d]
3196.8	(19/2)	$(17/2^+)$	879(1)	2(1)	
		$17/2^+$	1306.8(5)	4(1)	
3330.7	$21/2^+$	$21/2^+$	470.7(3)	2(1)	
		$17/2^+$	1440.5(4)	8(1)	0.87(14)
3727.6	$23/2^+$	$21/2^+$	397.0(2)	2(1)	
		$21/2^+$	867.4(1)	18(2)	0.61(6)
3992.9	$25/2^+$	$23/2^+$	265.3(1)	4(1)	0.55(7)
		$21/2^+$	1132.7(2)	16(2)	0.97(9)
4164.2	$(23/2^+)$	$21/2^+$	1303.9(5)	≈ 1	
4436.2	$25/2^+$	$(23/2^+)$	271.8(4)	≈ 1	
		$23/2^+$	708.6(3)	8(1)	0.45(6)
4461.1	$25/2^+$	$23/2^+$	733.5(3)	3(1)	0.48(11)
4963.2	$27/2^+$	$25/2^+$	502.5(6)	2(1)	
		$25/2^+$	970.3(3)	6(3)	0.94(5)[d]
5216.9	$(27/2^+)$	$25/2^+$	780.7(3)	3(1)	
5316.0	$29/2^+$	$(27/2^+)$	352.7(2)	2(1)	
		$25/2^+$	1323.2(4)	7(1)	1.1(2)
5668.2	$(29/2^+)$	$(27/2^+)$	451.3(3)	2(1)	
		$25/2^+$	1232(1)	2(1)	
6669	$(31/2^+)$	$29/2^+$	1353(1)	<1	
		$(27/2^+)$	1706(2)	2(1)	
6913	$(33/2^+)$	$(31/2^+)$	244(1)	<1	
		$29/2^+$	1597(1)	4(1)	
8834	$(37/2^+)$	$(33/2^+)$	1921(2)	≈ 1	

[a]Energy of the initial state.
[b]Uncertainty is given in parentheses in units of the last digit.
[c]Normalization.
[d]Value deduced for doublet.

tions at 1132.7 and 1323.2 keV. For the higher placed transitions at 1597 and 1921 keV no ratios could be deduced due to lack of statistics. The proposed spin assignments for their levels are based on systematics. Further, the previously highest placed 867.4 keV transition has a clear $\Delta I=1$ nature, as does the low-energy line at 265.3 keV. Thus, the spins within the region of the first band crossing are certain and a consistent picture emerges.

A weakly populated side structure has been found to feed into the $21/2^+$ and $23/2^+$ yrast states. The coincidence relations are clear and for the 708.6 keV line a DCO ratio of 0.45(6) has been deduced which is typical for a $\Delta I=1$ transition. It seems that this side structure is dominated by $\Delta I=1$ $M1$ transitions. γ-ray energies, relative intensities, and DCO ratios of transitions assigned to the positive-parity states in ^{83}Rb are compiled in Table I.

B. ^{85}Y

States in ^{85}Y were populated via the ^{59}Co(^{28}Si,2p) reaction at 99 MeV beam energy. The target consisted of a metallic Co foil with a thickness of 10.6 mg/cm^2. γ rays were detected with the FSU array of five Compton-suppressed Ge detectors of about 25% relative efficiency and a low-energy photon spectrometer (LEPS). Three Ge detectors and the

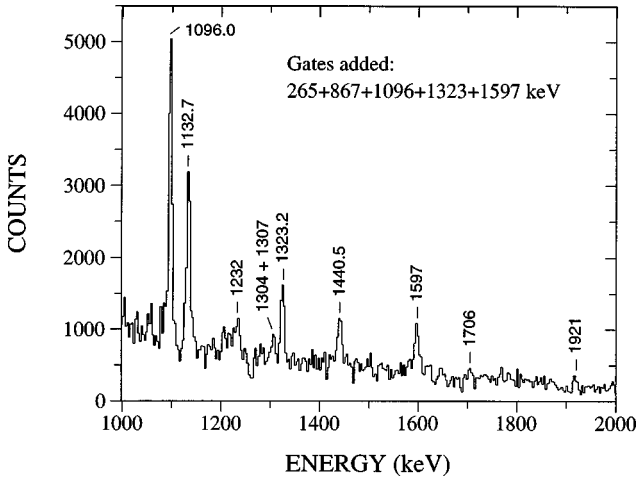

FIG. 3. Sum of several coincidence spectra of transitions in the positive-parity sequence of ^{83}Rb.

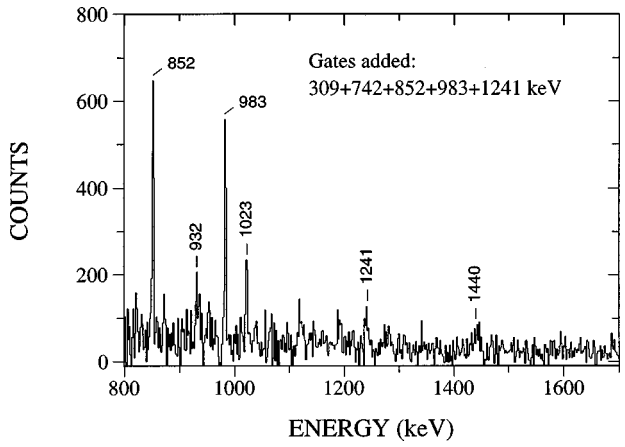

FIG. 4. Sum spectra of several clean coincidence gates for the positive-parity sequence in ^{85}Y.

LEPS were placed at 90° and two Ge detectors at 145° relative to the beam direction. A total of 5×10^7 events were collected on 8 mm tape and subsequently analyzed, mainly for the identification of high-spin states in ^{84}Y [17]. States in the much weaker ^{85}Y channel were identified through coincidences with known transitions of the positive-parity sequence [16]. A sum spectrum of several background-corrected coincidence spectra is shown in Fig. 4. The known transitions of the yrast sequence, such as the 852, 983, and 1241 keV lines, can be seen clearly. In addition, we found new transitions with energies of 309, 932, and 1440 keV. The 309 and 932 keV lines link a previously reported level at 4602 keV [16] to the yrast sequence. Thus a spin of $27/2^+$ is very likely for this state. The new 1440 keV transition tops the yrast band. No DCO ratios for the new transitions could be determined due to poor statistics. Thus all spins for the new ^{85}Y levels should be considered as tentative. The new transitions in ^{85}Y are shown in the level scheme compilation in Fig. 5.

III. DISCUSSION

A. Systematics of positive-parity states in $N=46$ isotones

There seems to be a great similarity between the excitation energies of the yrast states in the odd-proton nuclei with neutron number $N=46$, i.e., the energy separations of the positive-parity states in ^{83}Rb, ^{85}Y [16], ^{87}Nb [5,6], and ^{89}Tc [12] show common features, much more pronounced than among the chain of the odd-mass Rb isotopes. To illustrate this, a comparison of the positive-parity states among the $N=46$ odd-mass isotones is given in Fig. 5. Since only limited experimental results are known for ^{81}Br [22] this nucleus has not been included in the systematics. In all nuclei shown, a crossing between the 1qp and 3qp decay sequences at spin $21/2^+$ is observed. Previously, a loss of $E2$ collectivity at this spin has been inferred from lifetime measurements in ^{83}Rb [15], ^{85}Y [16], and ^{87}Nb [5] which supports the 1qp-3qp band-crossing scenario. After the band crossing, the $E2$ strength increases again to about $\geqslant 10$ and $\geqslant 12$ W.u. for the $29/2^+\rightarrow 25/2^+$ transitions in ^{85}Y [16] and ^{87}Nb [5], respectively, indicating similar collectivity in the 3qp bands. At the same time there is a systematic trend to smaller $E2$ transition energies within these bands with increasing proton number. In the heaviest $N=46$ nucleus, ^{89}Tc, states up to $(45/2^+)$ have been observed and interpreted in the framework of the

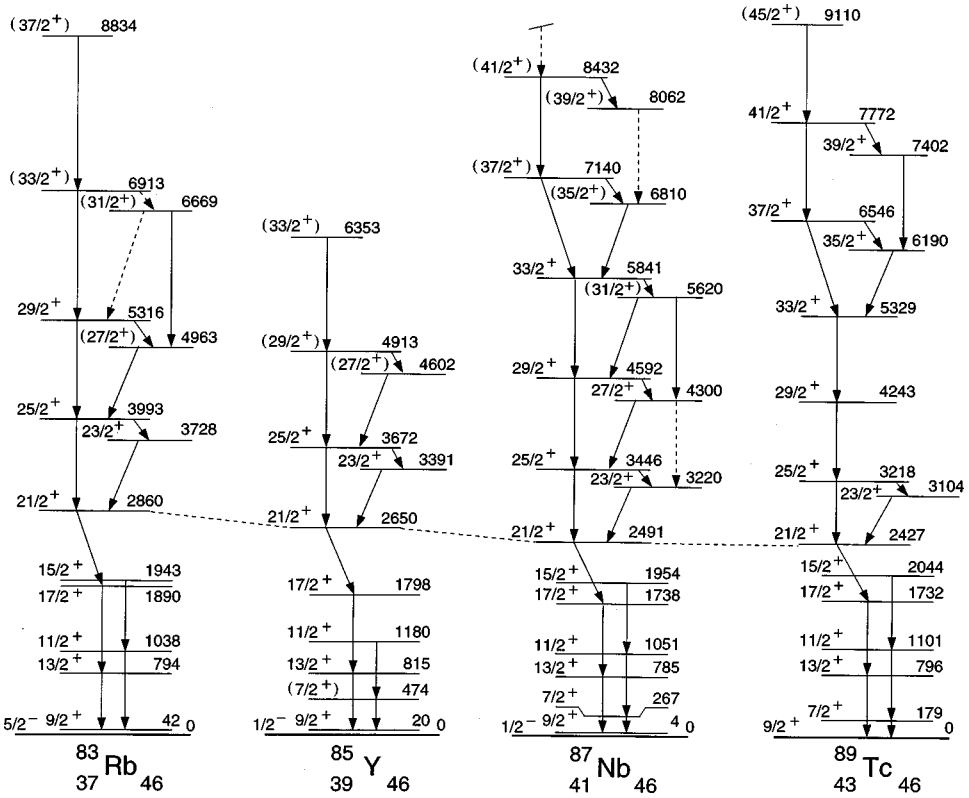

FIG. 5. Level schemes of positive-parity states in odd-proton $N=46$ nuclei. The experimental data have been taken from ^{85}Y, Ref. [16] and present work; ^{87}Nb, Ref. [5]; and ^{89}Tc, Ref. [12].

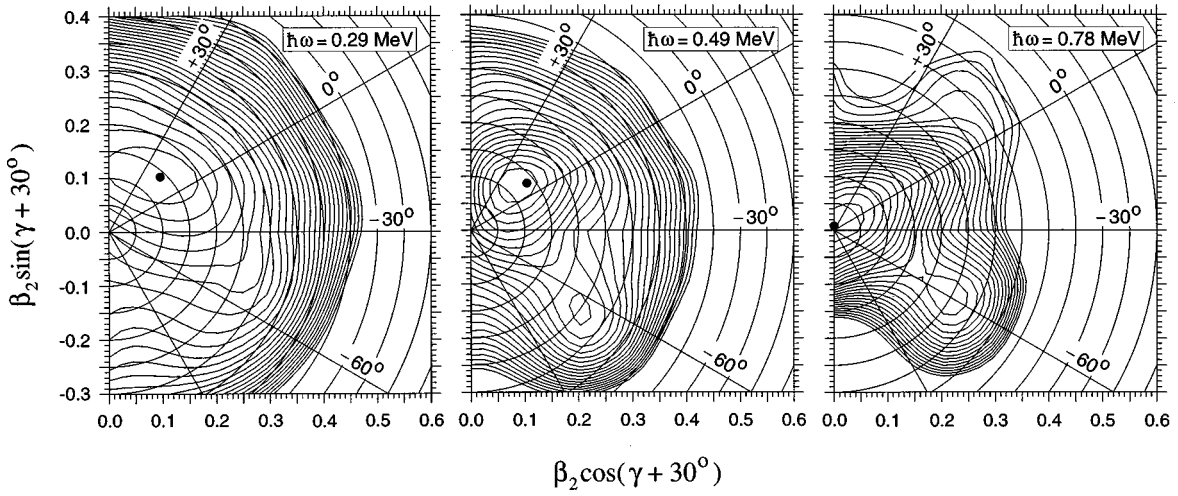

FIG. 6. Total Routhian surface plots in the (β_2, γ) polar coordinate system for the positive-parity configuration $(+,+1/2)$ in ^{83}Rb. The rotational frequencies are given in the inset. A collective prolate (oblate) shape is defined by $\gamma = 0°$ ($\gamma = -60°$). The contour lines are separated by 150 keV. The absolute minimum is given by a solid dot.

spherical shell model. $M1$ and $E2$ transition probabilities are not known. However, the interpretation of reduced collectivity in this nucleus is supported by the fair agreement of experimental and calculated level energies above the $21/2^+$ state.

B. Evolution of the nuclear shape in ^{83}Rb and other $N = 46$ isotones

The nucleus ^{83}Rb has been calculated to be almost spherical in its ground state, with a small quadrupole deformation of $\beta_2 = 0.071$ when a finite-range droplet macroscopic model and a folded-Yukawa single-particle microscopic model are used [23]. In the present work, the evolution of the nuclear shape has been studied as a function of the rotational frequency for the positive-parity states using total Routhian surface (TRS) calculations [24]. They have been performed with a Woods-Saxon potential for the single-particle motion and a short-range monopole paring force. Samples of these calculations are shown in Fig. 6 at different rotational frequencies for the configuration $(\pi, \alpha) = (+,+1/2)$ which has positive parity and signature $\alpha = +1/2$. At very low frequencies, the nucleus ^{83}Rb is calculated to be weakly deformed and very γ-soft, with a quadrupole deformation of about $\beta_2 = 0.13$ and a triaxiality parameter of $\gamma = +17°$. At a rotational frequency of 0.486 MeV (about spin $23/2^+$), a second minimum occurs which represents a well-deformed near-oblate shape with $\beta_2 = 0.25$ and $\gamma = -66°$. This second minimum persists up to high rotational frequencies. The calculated alignments indicate that the neutrons contribute most, i.e., the calculations support the alignment of a $g_{9/2}$ neutron pair in ^{83}Rb which drives the nucleus from a weakly deformed near-prolate shape to a medium deformed near-oblate shape. This situation reflects quite well the experimental findings (see Sec. III C 2).

Further, TRS shape calculations have also been performed for the positive-parity yrast states in the $N = 46$ odd-proton nuclei ^{81}Br, ^{85}Y, ^{87}Nb, and ^{89}Tc. The results (not displayed) show a strong variation of the nuclear shape as a function of the proton number. For low-spin states in ^{81}Br, a β_2- and γ-soft near-prolate ($\beta_2 \approx 0.16$) minimum, typical of the 1qp excitations, is predicted. This minimum is present in all isotones considered but gets stiffer and moves quickly towards a spherical shape with increasing proton number. After the first $g_{9/2}$ neutron crossing, a clear oblate-deformed shape emerges in ^{81}Br which is very similar to the ^{83}Rb shape shown in the middle panel of Fig. 6. In ^{85}Y, an oblate minimum is also calculated after the first neutron crossing, but less pronounced. For the ^{87}Nb and ^{89}Tc nuclei (above the $Z = 40$ subshell gap), oblate-deformed minima occur ($\beta_2 \approx 0.2$) weakly but fade away towards the spherical minimum with increasing rotational frequency.

C. Cranked shell-model analysis

1. Kinematic moments of inertia

To analyze the bands in the $N = 46$ isotones, the cranked shell model [25,26] has been applied where moments of inertia can be deduced as a function of the rotational frequency. In this model a rotation around a principal axis is assumed, and thus, the nucleus must exhibit at least a small

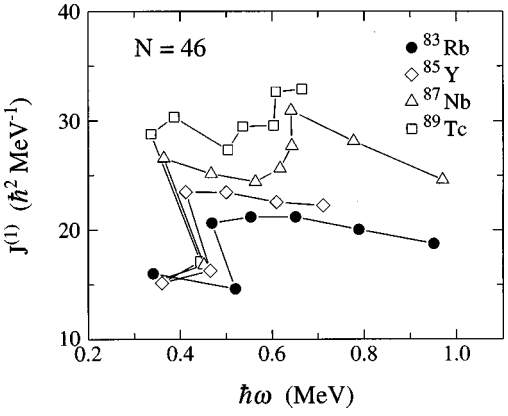

FIG. 7. Kinematic moments of inertia for the positive-parity yrast states in $N = 46$ isotones. In the analysis a value of $K = 5/2$ has been taken.

quadrupole deformation which seems to be justified by the TRS calculations presented before. The kinematic moments of inertia $J^{(1)}$ are shown in Fig. 7 for the yrast sequences with signature $\alpha = +1/2$ in ^{83}Rb and other $N = 46$ isotones. The first back bending in ^{83}Rb happens at a rotational frequency of about 0.50 MeV, slightly higher when compared to 0.44 MeV in ^{85}Y and ^{87}Nb. The first crossing systematics indicate a common underlying structure, i.e., the first crossing in ^{83}Rb is based on the breaking of a $g_{9/2}$ neutron pair, very similar to the discussion in ^{85}Y [16] and the magnetic-moment results for ^{87}Nb [7,8].

At higher frequencies, the moments of inertia in ^{83}Rb show an almost constant behavior. This indicates a collective nature of the yrast states involved. On the other hand, in ^{87}Nb and ^{89}Tc a second upbend occurs at a frequency of 0.63 MeV, establishing a distinct difference to the lower mass isotones in the $N = 46$ chain. The nature of this second upbend is not well understood yet. It happens around spin $37/2^+$ in ^{87}Nb and ^{89}Tc, just above the spin range accessible in our ^{83}Rb study. A possible explanation is proposed on the basis of shape changes and calculated crossing frequencies (see Sec. III C 3).

2. Alignment and signature splitting

The aligned angular momentum i_x has been extracted using the cranked shell-model approach. It is shown in Fig. 8 (top panel) as a function of the rotational frequency for the favored ($\alpha = +1/2$) positive-parity decay sequences in ^{83}Rb and other isotones. A collective rotor with two Harris parameters has been taken as rotational reference. The parameter values chosen are in the range typical for this mass region [3]. They have been fine tuned in such a way that the aligned angular momenta for the high-spin 3qp extension of the ^{83}Rb decay sequence approaches an almost constant value. The same reference has been used for the analysis of the decay sequences in the heavier $N = 46$ isotones, which also leads to a constant alignment for the three highest points in ^{87}Nb.

As it can be seen from the moments of inertia, no second alignment occurs in ^{83}Rb up to a rotational frequency of 0.95 MeV. In contrast, a strong upbend can be seen in ^{87}Nb at 0.65 MeV. In ^{89}Tc, a multistep upbend occurs in the frequency range 0.5 to 0.6 MeV. The strong upbends in ^{87}Nb and ^{89}Tc lead to an alignment gain of about 6 $\hbar$ which might be explained by the partial (second) alignment of a $g_{9/2}$ proton pair since the first alignment is Pauli-blocked in these odd-proton isotones. It is interesting to note that the second upbend occurs in the yrast sequence of nuclei with more than 40 protons, i.e., for nuclei above the spherical subshell gap at $Z = 40$. Assuming a partial $g_{9/2}$ proton alignment, the second upbend reflects the successive filling of the $g_{9/2}$ proton orbitals, because more than one $g_{9/2}$ proton is required to explain this effect.

It was found in previous cranked shell-model calculations [3,27,28] that when the Fermi level is in the upper half of the intruder $g_{9/2}$ neutron subshell the alignment of a pair of $g_{9/2}$ neutrons drives the nucleus to an oblate shape and a significant signature splitting remains in the 3qp band when compared with the 1qp excitations. This is in contrast to the situation found for aligning $g_{9/2}$ protons in the mass 80 region (the Fermi level is at the beginning of the $g_{9/2}$ subshell) where a prolate shape and a vanishing signature splitting are predicted.

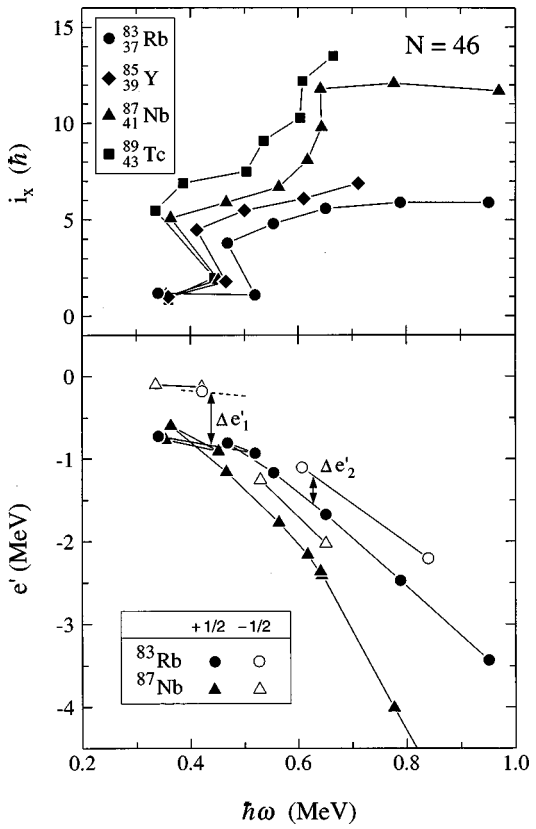

FIG. 8. Top: Aligned angular momentum i_x for the favored ($\alpha = +1/2$) positive-parity sequences in some $N = 46$ isotones. Bottom: Energy in the rotating frame for the positive-parity states in ^{83}Rb and ^{87}Nb. Solid (open) symbols have been used for the favored (unfavored) decay sequence. The signature splitting before ($\Delta e'_1$) and after ($\Delta e'_2$) the first crossing has been indicated. The unfavored sequences are divided into two curves because the first $19/2^+$ state in ^{83}Rb is uncertain and not known in ^{87}Nb. In both graphs a rotor with the Harris parameters $J_0 = 12.5\,\hbar^2/\mathrm{MeV}$ and $J_1 = 0.0\,\hbar^4/\mathrm{MeV}^3$ has been used as reference. A value of $K = 5/2$ has been used in the analysis.

The energies in the rotating frame for the two signature partner sequences in ^{83}Rb are shown in Fig. 8 (bottom panel) along with the values for ^{87}Nb. For the unfavored ($\alpha = -1/2$) 1qp configuration in ^{83}Rb only one data point is available since the $7/2^+$ state at 805.0 keV [13] is not linked by an $E2$ transition to the $11/2^+$ state and the parity of the 19/2 level at 3196.8 keV is uncertain. With this limited information, a signature splitting $\Delta e'_1 = e'(\alpha = -1/2) - e'(\alpha = +1/2)$ of about 640 keV has been estimated at a rotational frequency of 440 keV, while for the 3qp band the signature splitting $\Delta e'_2$ is reduced to about 360 keV at a frequency above 620 keV. The reductions in ^{83}Rb and ^{87}Nb are somewhat similar but not as dramatic as in the odd-neutron nuclei ^{79,81}Kr [28,29], where the signature splitting disappears completely after the alignment of a $g_{9/2}$ proton pair, e.g., see Fig.

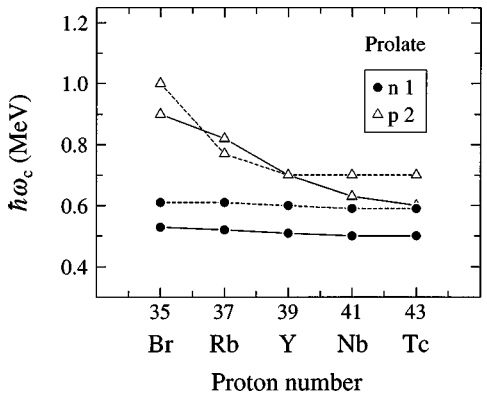

FIG. 9. First $g_{9/2}$ neutron (full circle) and second $g_{9/2}$ proton (open triangle) crossing frequencies as a function of the proton number. The values have been calculated with the cranked shell model for a prolate deformed shape with $\beta_2=0.15$ (full line) and $\beta_2=0.20$ (dashed line). The hexadecapole deformation β_4 has been set to zero in the calculations.

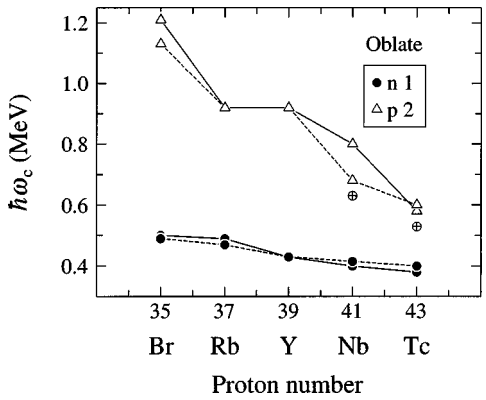

FIG. 10. First $g_{9/2}$ neutron (full circle) and second $g_{9/2}$ proton (open triangle) crossing frequencies as a function of the proton number. The values have been calculated with the cranked shell model for an oblate deformed shape with a constant deformation of $\beta_2=0.20$ (dashed line) and a variable quadrupole deformation (full line). The following deformations (β_2) have been assumed: ^{81}Br (0.25), ^{83}Rb (0.25), ^{85}Y (0.20), ^{87}Nb (0.15), and ^{89}Tc (0.10). The hexadecapole deformation β_4 has been set to zero. Experimental values for the second crossings in ^{87}Nb and ^{89}Tc are shown by encircled plus signs.

6 in Ref. [29]. Cranked shell-model calculations support qualitatively the observed splittings. For the 1qp structure, a signature splitting of about 710 keV has been calculated at a similar frequency with a prolate shape of $\beta_2=0.15$. A change of the triaxiality parameter to positive values increases the calculated splitting while for slightly negative values ($\gamma\approx-15°$) a better agreement with the experimental value is obtained. For the 3qp structure, a splitting of 150 keV is predicted by our calculations at a frequency of 650 keV when a perfect oblate shape with $\beta_2=0.25$ is assumed. A small reduction of the triaxiality parameter to $\gamma=-50°$ improves the agreement with the experimental value. In summary, the behavior in ^{83}Rb can clearly be related to the alignment of a $g_{9/2}$ neutron pair which drives the nucleus to a near-oblate shape.

3. Calculation of crossing frequencies

Using the cranked shell model, crossing frequencies $\hbar\omega_c$ have been calculated for the first $g_{9/2}$ neutron and the second $g_{9/2}$ proton crossings as a function of the proton number for different deformations. For the one-quasiproton excitations in ^{83}Rb and ^{85}Y an average quadrupole deformation of about $\beta_2=0.15$ can be deduced from the known $E2$ transition probabilities, and a near-prolate shape is suggested by our TRS calculations. A somewhat higher deformation of about $\beta_2=0.21$ has been extracted for the 1qp excitations in ^{87}Nb [5]. Thus crossing frequencies have been calculated for such prolate deformed shapes and the results are shown in Fig. 9 for some $N=46$ isotones. For the case of constant deformation, the first neutron crossing frequency is almost constant but somewhat higher than the experimental values. An increase in deformation from 0.15 to 0.20 shifts the first neutron crossing frequency to higher values as displayed in Fig. 9.

The aligning neutrons, however, induce a shape change from a near-prolate to a near-oblate shape, and thus, a strong variation of the neutron crossing frequency is expected. Therefore, the crossing frequency has also been calculated for an oblate deformed shape which is suggested by our TRS calculations and typical for the 3qp configuration. These calculations have been carried out with (i) decreasing quadrupole deformation when going towards the heavier isotones as predicted by our TRS calculations, and (ii) with a constant deformation of $\beta_2=0.20$. The results are shown in Fig. 10. The first neutron crossing frequency decreases slightly with increasing proton number and underestimates the experimental results. A reasonable estimate would be the average value extracted from the 1qp (prolate) and the 3qp (oblate) cases which results for ^{83}Rb in $(0.52+0.49)/2\,\mathrm{MeV}=0.505\,\mathrm{MeV}$ in good agreement with the experimental value of 0.50 MeV. In this approximation also the experimental trend of decreasing crossing frequency with increasing proton number can be well reproduced.

The question remains about the second alignments seen in ^{87}Nb and ^{89}Tc but not present in ^{83}Rb up to a rotational frequency of 0.95 MeV. Our conjecture is that the second $g_{9/2}$ proton crossing might be responsible (the first $g_{9/2}$ proton crossing is Pauli-blocked in an odd-proton nucleus). Thus, cranked shell-model calculations have been carried out for a near-oblate deformed shape and the results are shown in Fig. 10 along with the extracted experimental values. The graph demonstrates that the second $g_{9/2}$ proton crossing frequency increases dramatically when going towards smaller proton numbers. This trend is almost independent on the specific amount of deformation and mainly reflects the reduced occupation of the $g_{9/2}$ proton orbitals. Hence, a very delayed second crossing in ^{81}Br, ^{83}Rb, and ^{85}Y is predicted in qualitative agreement with the experimental situation. But the calculated frequencies are still somewhat too small to reproduce the nonobservation of any second crossing in ^{83}Rb, and slightly too high for the heavier isotones when compared with the experimental values.

D. Side structure in ^{83}Rb

A side structure has been identified in ^{83}Rb which feeds into the $23/2^+$ and $25/2^+$ states. The strongest transitions in this weakly populated structure are $\Delta I=1$ transitions, such as the 708.6 and 780.7 keV lines. These states may reflect shell-model influence. In the heavier nucleus ^{85}Rb [1,2] the positive-parity yrast sequence above the $21/2^+$ state is comprised of fast $\Delta I=1$ $M1$ transitions with $M1$ strengths of up to 1.2 W.u. States up to spin $25/2^+$ in ^{85}Rb have been interpreted as a seniority 3 configuration resulting from the coupling of a $g_{9/2}$ neutron pair to the unpaired $g_{9/2}$ proton. For higher positive-parity yrast states (up to $33/2^+$) the additional breaking of a $g_{9/2}$ proton pair has been suggested, leading to a seniority 5 configuration. Hence, the comparison indicates that in the transitional nucleus ^{83}Rb spherical shell-model states may be present but as nonyrast excitations, while the yrast sequence itself is formed by collective excitations.

IV. SUMMARY AND CONCLUSIONS

High-spin states in the odd-proton nucleus ^{83}Rb were populated via the ^{68}Zn(^{18}O,$p2n$) reaction at 56 MeV beam energy, and in ^{85}Y via the ^{59}Co(^{28}Si,$2p$) reaction at 99 MeV. The known yrast sequences of positive parity in ^{83}Rb and ^{85}Y have been extended up to states with spins of $(37/2^+)$ and $(33/2^+)$, respectively, i.e., through the region of the first band crossing which occurs around spin $21/2^+$. Total Routhian shape calculations, crossing frequencies calculated with the cranked shell model, systematics of $N=46$ isotones, and Pauli blocking of the first $g_{9/2}$ proton crossing indicate that the band crossing at spin $21/2^+$ in ^{83}Rb is related to the alignment of a $g_{9/2}$ neutron pair. The properties of the yrast states above spin $21/2^+$ in ^{83}Rb can be attributed to a collective 3qp band, $\pi g_{9/2}\otimes(\nu g_{9/2})^2$.

The 3qp band in ^{83}Rb exhibits a reduced signature splitting when compared to the lower-lying 1qp sequence which is in agreement with predictions by the cranked shell model for a near-oblate deformed shape. No second alignment has been seen in the 3qp band, in contrast to the yrast sequences of the heavier $N=46$ odd-proton nuclei ^{87}Nb and ^{89}Tc. This behavior in ^{83}Rb can be related to the occurrence of a well-deformed oblate shape and the fact that for $Z=37$ more energy is needed to break a $g_{9/2}$ proton pair. The situation seems to be present also in the positive-parity states of ^{85}Y ($Z=39$) while a different picture unfolds for the yrast states in ^{87}Nb ($Z=41$) and ^{89}Tc ($Z=43$), i.e., above the $Z=40$ spherical subshell gap.

ACKNOWLEDGMENTS

The authors thank J. X. Saladin for the loan of the Pittsburgh Ge detectors and electronics used for the joint Pittsburgh–Florida State Universities detector array. The authors are grateful to S. Frauendorf, R. Schwengner, and H. Schnare for fruitful discussions and to W. Nazarewicz and R. Wyss for providing the TRS and CSM computer codes. This work was supported by the National Science Foundation under Grant No. PHY-92-10082 with Florida State University and under Grant No. PHY-94-02761 with the University of Notre Dame.

[1] G. Winter, J. Döring, F. Dönau, and L. Funke, Z. Phys. A **334**, 415 (1989).

[2] R. Schwengner, G. Winter, J. Reif, H. Prade, L. Käubler, R. Wirowski, N. Nicolay, S. Albers, S. Eßer, P. von Brentano, and W. Andrejtscheff, Nucl. Phys. **A584**, 159 (1995).

[3] S. L. Tabor, P. D. Cottle, C. J. Gross, U. J. Hüttmeier, E. F. Moore, and W. Nazarewicz, Phys. Rev. C **39**, 1359 (1989).

[4] J. Döring, R. Schwengner, L. Funke, H. Rotter, G. Winter, B. Cederwall, F. Lidén, A. Johnson, A. Atac, J. Nyberg, and G. Sletten, Phys. Rev. C **50**, 1845 (1994).

[5] A. Jungclaus, K. P. Lieb, C. J. Gross, J. Heese, D. Rudolph, D. J. Blumenthal, P. Chowdhury, P. J. Ennis, C. J. Lister, C. Winter, J. Eberth, S. Skoda, M. A. Bentley, W. Gelletly, and B. J. Varley, Z. Phys. A **340**, 125 (1991).

[6] B. J. Min, S. Suematsu, S. Mitarai, T. Kuroyanagi, K. Heiguchi, and M. Matsuzaki, Nucl. Phys. **A530**, 211 (1991).

[7] M. Weiszflog, J. Billowes, J. Eberth, C. J. Gross, M. K. Kabadiyski, K. P. Lieb, T. Mylaeus, and D. Rudolph, Nucl. Phys. **A584**, 133 (1995).

[8] A. Jungclaus, C. Teich, V. Fischer, D. Kast, K. P. Lieb, C. Lingk, C. Ender, T. Härtlein, F. Köck, D. Schwalm, J. Billowes, J. Eberth, and H. G. Thomas, Phys. Rev. Lett. **80**, 2793 (1998).

[9] C. Broude, E. Dafni, A. Gelberg, M. B. Goldberg, G. Goldring, M. Hass, O. C. Kistner, and A. Zemel, Phys. Lett. **105B**, 119 (1981).

[10] A. I. Kucharska, J. Billowes, and C. J. Lister, J. Phys. G **15**, 1039 (1989).

[11] A. W. Mountford, T. Vass, G. Kumbartzki, L. A. Bernstein, N. Benczer-Koller, R. Tanczyn, C. J. Lister, P. Chowdhury, and S. J. Freeman, Phys. Rev. C **51**, 513 (1995).

[12] D. Rudolph, A. Harder, T. D. Johnson, K. P. Lieb, R. Schubart, D. Foltescu, H. A. Roth, Ö. Skeppstedt, I. G. Bearden, T. Shizuma, G. Sletten, H. Grawe, J. Persson, and D. Seweryniak, Nucl. Phys. **A587**, 181 (1995).

[13] W. Gast, K. Dey, A. Gelberg, U. Kaup, F. Paar, R. Richter, K. O. Zell, and P. von Brentano, Phys. Rev. C **22**, 469 (1980).

[14] R. B. Firestone and V. S. Shirley, *Table of Isotopes*, 8th ed. (Wiley and Sons, New York, 1996).

[15] U. I. Zhovliev, V. G. Kiptilyi, M. F. Kudoyarov, I. Kh. Lemberg, A. I. Muminov, A. A. Pasternak, and L. A. Rassadin, Izv. Akad. Nauk SSSR, Ser. Fiz. **49**, 2096 (1985).

[16] R. Diller, K. P. Lieb, L. Lühmann, T. Osipowicz, P. Sona, B. Wörmann, L. Cleemann, and J. Eberth, Z. Phys. A **321**, 659 (1985).

[17] J. Döring *et al.* (unpublished).

[18] S. L. Tabor, M. A. Riley, J. Döring, P. D. Cottle, R. Books, T. Glasmacher, J. W. Holcomb, J. Hutchins, G. D. Johns, T. D.

Johnson, T. Petters, O. Tekyi-Mensah, P. C. Womble, L. Wright, and J. X. Saladin, Nucl. Instrum. Methods Phys. Res. B **79**, 821 (1993).
[19] K. S. Krane, R. M. Steffen, and R. M. Wheeler, Nucl. Data Tables **11**, 351 (1973).
[20] A. Krämer-Flecken, T. Morek, R. M. Lieder, W. Gast, G. Hebbinghaus, H. M. Jäger, and W. Urban, Nucl. Instrum. Methods Phys. Res. A **275**, 333 (1989).
[21] J. Döring, D. Ulrich, G. D. Johns, M. A. Riley, and S. L. Tabor, Phys. Rev. C **59**, 71 (1999).
[22] L. Funke, J. Döring, P. Kemnitz, P. Ojeda, R. Schwengner, E. Will, G. Winter, A. Johnson, L. Hildingsson, and T. Lindblad, Z. Phys. A **324**, 127 (1986).
[23] P. Möller, J. R. Nix, W. D. Myers, and W. J. Swiatecki, At. Data Nucl. Data Tables **59**, 185 (1995).
[24] W. Nazarewicz, J. Dudek, R. Bengtsson, T. Bengtsson, and I. Ragnarsson, Nucl. Phys. **A435**, 397 (1985).
[25] R. Bengtsson and S. Frauendorf, Nucl. Phys. **A327**, 139 (1979).
[26] R. Bengtsson, S. Frauendorf, and F.-R. May, At. Data Nucl. Data Tables **35**, 15 (1986).
[27] S. Frauendorf and F. R. May, Phys. Lett. **125B**, 245 (1983).
[28] L. Funke, J. Döring, P. Kemnitz, E. Will, G. Winter, A. Johnson, L. Hildingsson, and T. Lindblad, Nucl. Phys. **A455**, 206 (1986).
[29] G. D. Johns, J. Döring, J. W. Holcomb, T. D. Johnson, M. A. Riley, G. N. Sylvan, P. C. Womble, V. A. Wood, and S. L. Tabor, Phys. Rev. C **50**, 2786 (1994).